

## ORIGINAL ARTICLE

# Quantifying the size-resolved dynamics of indoor bioaerosol transport and control

S. A. Kunkel<sup>1</sup> | P. Azimi<sup>1</sup> | H. Zhao<sup>1</sup> | B. C. Stark<sup>2</sup> | B. Stephens<sup>1</sup> 

<sup>1</sup>Department of Civil, Architectural and Environmental Engineering, Illinois Institute of Technology, Chicago, IL, USA

<sup>2</sup>Department of Biology, Illinois Institute of Technology, Chicago, IL, USA

## Correspondence

Brent Stephens, Department of Civil, Architectural, and Environmental Engineering, Illinois Institute of Technology, Chicago, IL, USA.

Email: brent@iit.edu

## Funding information

Alfred P. Sloan Foundation, Grant/Award Number: G-2013-5-25 MBPF; ASHRAE New Investigator Award

## Abstract

Understanding the bioaerosol dynamics of droplets and droplet nuclei emitted during respiratory activities is important for understanding how infectious diseases are transmitted and potentially controlled. To this end, we conducted experiments to quantify the size-resolved dynamics of indoor bioaerosol transport and control in an unoccupied apartment unit operating under four different HVAC particle filtration conditions. Two model organisms (*Escherichia coli* K12 and bacteriophage T4) were aerosolized under alternating low and high flow rates to roughly represent constant breathing and periodic coughing. Size-resolved aerosol sampling and settle plate swabbing were conducted in multiple locations. Samples were analyzed by DNA extraction and quantitative polymerase chain reaction (qPCR). DNA from both organisms was detected during all test conditions in all air samples up to 7 m away from the source, but decreased in magnitude with the distance from the source. A greater fraction of T4 DNA was recovered from the aerosol size fractions smaller than 1  $\mu\text{m}$  than *E. coli* K12 at all air sampling locations. Higher efficiency HVAC filtration also reduced the amount of DNA recovered in air samples and on settle plates located 3–7 m from the source.

## KEYWORDS

aerosol, bioaerosol, coughing, infectious disease transmission, pathogen, respiratory activities

## 1 | INTRODUCTION

Communicable respiratory illnesses lead to large expenses associated with health care, absence from work, and lost worker productivity.<sup>1</sup> Several complex physical and biological processes govern the transmission of respiratory pathogens and the associated risk of infection to occupants in indoor environments. When a person breathes, speaks, sneezes, or coughs, particles of various sizes are expelled.<sup>2–7</sup> These particles consist of water, proteins, salts, and various organic and inorganic matter, and if the person has a communicable respiratory infection, also smaller bacterial or viral particles.<sup>8–10</sup> The largest particles (ie, “droplets”) rapidly deposit onto nearby people and/or surfaces, leading to potential direct spray, direct contact, or fomite transmission.<sup>11–15</sup> The emitted particles will also rapidly evaporate into smaller “droplet nuclei” particles that can remain suspended in the air for long periods of time and transport long distances.<sup>16</sup> Previous studies suggest that liquid droplet evaporation occurs rapidly, typically

within less than a few seconds after emission, depending on the original particle size and ambient thermodynamic conditions.<sup>9,17,18</sup>

Human pathogens that are known to be transmitted at least partially via the airborne route include a number of viral, bacterial, and fungal species. Among the known airborne transmitted viruses are those that cause measles, mumps, chicken pox, influenza, SARS, and the common cold.<sup>19–23</sup> These include viruses with DNA genomes as well as both plus- and minus-strand RNA genomes. Among the known airborne transmitted bacteria are *Streptococcus pyogenes*, *Neisseria meningitidis*, *Corynebacterium diphtheriae*, *Mycobacterium tuberculosis*, and *Bordetella pertussis*.<sup>24,25</sup>

Although transmission pathways and means of controlling the transmission of communicable airborne diseases have been studied for more than a century, several fundamental questions remain unanswered. For example, influenza transmission is one of the most widely studied communicable airborne diseases. However, it is still not clear which routes of transmission (ie, fomite contact, direct droplet spray,

or inhalation of long-range droplet nuclei) are dominant<sup>13,20,22</sup> or what strategies are the most effective ways of reducing influenza transmission risks.<sup>23,26</sup> Viable influenza viruses and influenza virus RNA have been detected in the effluent air from breathing and coughing subjects and in indoor air samples in a number of recent studies,<sup>27-34</sup> which suggests that long-range aerosol transport may be an important influenza transmission pathway. Further, commonly available particle filters in recirculating HVAC systems are thought to be useful for reducing the transmission risk of a number of airborne infectious diseases,<sup>23,35-40</sup> but key questions still remain about the effectiveness of particle filtration for controlling airborne infectious aerosol transport.

To further elucidate the mechanisms of transport and control of airborne infectious diseases, a number of studies have used aerosolized surrogate organisms to mimic the dynamics of bacterial and viral particles in the indoor environment. For example, manikins and cough simulators have recently been developed and used to mimic the aerosol dynamics of influenza virus transmission in simulated indoor settings.<sup>41-43</sup> Others have used surrogates such as bacteriophage MS2, *Mycobacterium vaccae*, and *Escherichia coli* to mimic the aerosol dynamics of viral and bacterial pathogens.<sup>44-46</sup> However, few of these studies have used surrogate aerosolization in realistic indoor environments to explore the size-resolved bioaerosol transport dynamics or the impact of potential control strategies such as HVAC particle filtration.

Here, we report on a series of experiments conducted in an unoccupied apartment unit in which we aerosolized model organisms as surrogates for human pathogens and quantified their dispersion in multiple locations under different HVAC filtration conditions. We used (i) *Escherichia coli* K12, a Gram-negative bacterium (characteristic size  $\sim 0.5 \mu\text{m} \times \sim 2 \mu\text{m}$ ), as a model for pathogens such as *Bordetella* and *Neisseria*, and (ii) bacteriophage T4, a double-stranded DNA coliphage (characteristic size  $\sim 90 \text{ nm} \times \sim 200 \text{ nm}$ ), as a model for pathogens such as norovirus and influenza virus. Size-resolved aerosol sampling and settle plate swabbing were conducted in multiple locations, and samples were analyzed by DNA extraction and quantitative polymerase chain reaction (qPCR). Results are intended to provide quantitative insight into the aerosol dynamics of pathogen transmission in indoor environments.

## 2 | MATERIALS AND METHODS

### 2.1 | Bioaerosol emissions procedure

Model organisms were aerosolized under alternating low and high flow rates to roughly represent constant breathing and periodic coughing, respectively. A High-output Extended Aerosol Respiratory Therapy (HEART) Lo-Flo nebulizer (Mini-HEART, Westmed, Inc., Tucson, AZ, USA) was used for constant low-flow emissions, and an air compressor (California Air Tools CAT-1610A, San Diego, CA, USA) was used to produce periodic high flow emissions through the same nebulizer. Both devices were connected via 10-mm-diameter tubing to the same mixing chamber comprising a 200 mm length of 25-mm-diameter metal pipe. The end of the 25-mm-diameter mixing

#### Practical Implications

To our knowledge, this is one of the first studies to experimentally quantify the size-resolved bioaerosol dynamics of surrogate microorganisms aerosolized in a realistic indoor environmental setting under different HVAC filtration conditions. The results provide insight into how the size-resolved aerosol dynamics of potentially pathogenic organisms emitted from respiratory activities may influence their transmission and control in indoor environments.

chamber also served as the circular output orifice. An electronically actuated switching valve was used with a timer to cycle between each flow condition. For each test condition, the nebulizer operated continuously to roughly represent continuous breathing, and the air compressor ran for 15 s every 5 min to roughly represent periodic higher flow coughing.

The mean ( $\pm$ SD) volumetric flow rate under the low-flow condition was measured to be  $\sim 0.13 (\pm 0.02)$  L/s using a TSI Model 4043 mass flow meter. The volumetric flow rate under the high-flow condition was measured by placing a smooth 1-m-long tube on the output orifice to achieve an approximately uniform airflow cross-sectional velocity profile at the end of the tube. The cross-sectional velocity was measured at the end of the tube using a Fluke 975 AirMeter anemometer. The mean ( $\pm$ SD) volumetric airflow rate was estimated to be  $\sim 10 (\pm 1)$  L/s by multiplying the cross-sectional area of the tube by the measured air velocity. Both flow rates are considered to be reasonably in range with previous measurements of average flow rates during breathing<sup>4,5</sup> and coughing<sup>47-50</sup> by adult human subjects and are similar to those used in a recently developed cough simulator.<sup>51</sup> However, the concentration of model organisms loaded into the nebulizer did not vary with flow rate and the simulated breathing flow rate was somewhat lower than the 0.17-0.18 L/s recommended in ISO/TS Standard 16976-1.<sup>52</sup> Therefore, the bioaerosol emissions procedure herein should not be considered an exact replicate of human respiratory activities but rather represents an attempt to aerosolize sufficient mass of model organisms for subsequent collection, extraction, and analysis with bulk airflow rates and particle size distributions that are reasonably consistent with human breathing and coughing.

To evaluate the size-resolved particle distributions resulting from the bioaerosol emissions procedure, measurements were conducted in an enclosed room using a TSI NanoScan Scanning Mobility Particle Sizer (SMPS, TSI NanoScan Model 3910, Shoreview, MN, USA) and a TSI Optical Particle Sizer (OPS, TSI Model 3330, Shoreview, MN, USA). Measurements were conducted during a 2-h background concentration period followed by a 2-h measurement period with the bioaerosol emission source operating normally. Measurements were made  $\sim 0.3 \text{ m}$  and  $\sim 3 \text{ m}$  away from the outlet orifice and were repeated twice with each of the two model organisms loaded in the nebulizer separately. Results were compared to those from human expiratory emissions measurements in the literature using similar instrumentation and methods.<sup>42,51</sup>

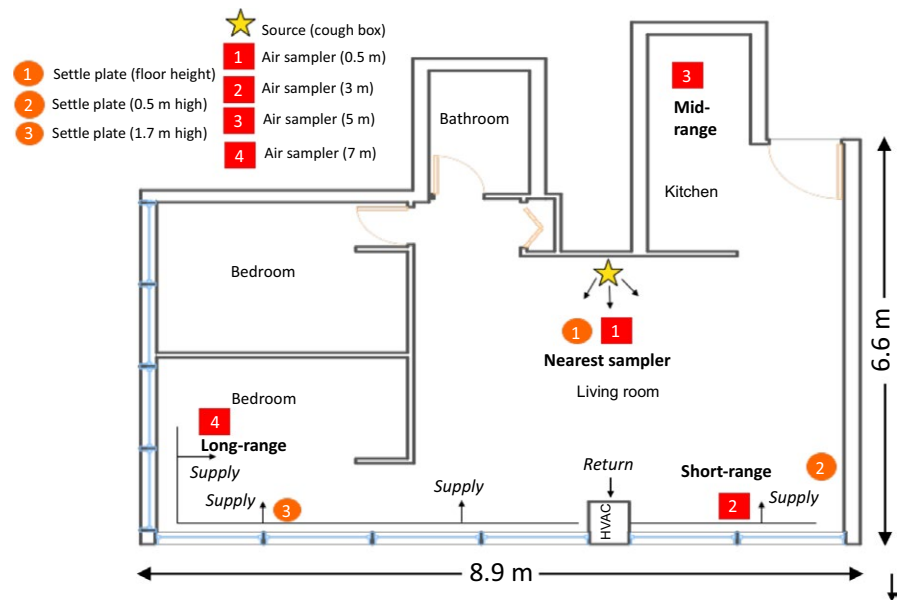


**FIGURE 1** Layout of the unoccupied test space with air sampling locations in red, settle plate sampling locations in orange, and the bioaerosol emission source in yellow. Supply ductwork and registers as well as the return plenum are noted with arrows

## 2.2 | Test space description and experimental setup

Measurements were conducted from January 2015 to January 2016 in *studioE* (the Suite for Testing Urban Dwellings and their Indoor and Outdoor Environments), a  $\sim 150\text{-m}^3$  unoccupied apartment unit on the third floor of a graduate student dormitory on the campus of Illinois Institute of Technology in Chicago, IL (Figure 1). Full details regarding this unit are described elsewhere.<sup>53</sup> Briefly, there is a central 100% recirculating air-handling unit that is connected to a rigid sheet metal ductwork installed within conditioned space, but it is not connected to any heating or cooling system. There is one  $40\text{ cm} \times 64\text{ cm}$  return grille located at the plenum on the bottom of the top-flow air-handling unit where a filter can be installed. There are four supply registers along the supply ductwork, but there is no return ductwork.

Tests were conducted under four different HVAC filter conditions: (i) no filter, (ii) with a 10-cm-deep MERV 8 Airguard filter, (iii) with a 10-cm-deep MERV 11 Airguard filter, and (iv) with a 12.7-cm-deep Healthy Solutions Climate MERV 16 filter. The central HVAC system was operated continuously throughout each test period at airflow rates of approximately 1720, 1680, 1640, and 1620  $\text{m}^3/\text{h}$  for under the no filter, MERV 8, MERV 11, and MERV 16 filter conditions, respectively. These airflow rates correspond to recirculation rates ranging from 10.8 to 11.5 per h, which are 40–50% higher than the average seen in typical residential and light-commercial buildings (although not out of the realm of possibility for similar spaces).<sup>54</sup> However, it should be noted that the higher recirculation rates in this study are likely to increase the impact that HVAC filtration would have compared to a system with lower recirculation rates. The pressure drops measured across the three filters were 29, 37, and 31 Pa, respectively. The in situ size-resolved removal efficiencies of the three filters were measured by elevating particle concentrations through a combination of burning incense and operating a TSI Model 8026 particle generator with water and NaCl in solution and alternately measuring the upstream and downstream concentrations, as reported in a previous study<sup>55</sup> and shown in Figure 2.

## 2.3 | Growth and cultivation of model organisms

Each organism and HVAC filtration condition were tested separately and in triplicate, which yielded a total of 24 experiments. Bacteriophage T4 and its host *Escherichia coli* K12 were obtained from existing frozen stocks at Illinois Institute of Technology (Chicago, IL). Culture media and all other reagents were previously purchased from Difco Laboratories (Detroit, MI, USA). *E. coli* K12 was cultivated in trypticase soy broth (TSB) and plated on trypticase soy agar (TSA), both at  $37^\circ\text{C}$ . Enumeration of bacteriophage T4 was accomplished by cultivation on its *E. coli* host using the top agar overlay method. The *E. coli* was incubated for 6 h at  $37^\circ\text{C}$  with gentle shaking. Simultaneously 4-mL

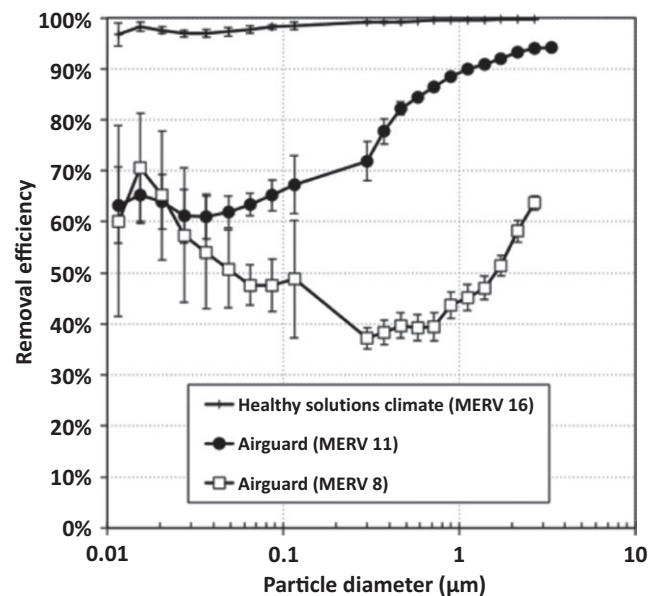


**FIGURE 2** Size-resolved in situ particle removal efficiency of the three HVAC filters tested herein. Data are from Fazli and Stephens (2016)<sup>55</sup>

tubes of TSA containing 0.6% agar were melted and kept in a 42°C water bath. Previously prepared 1.5% TSA petri dishes were allowed to warm to room temperature before use. Then, a series of 10-fold dilutions of T4 were prepared in TSB, and 0.7 mL of each dilution was added to each of the tempered 4-mL TSA tubes, after which 0.3 mL of *E. coli* was added and the mixture quickly vortexed and poured over the TSA plates. Upon solidification of the top agar, the plates were then inverted and incubated overnight at 37°C, and the following day, plaque-forming units (PFU) were counted.

High titer T4 lysate was produced through a modified protocol used in our laboratory. Plates containing a sufficient amount of PFUs (ie, >100) were used. First, 2-3 drops of  $\text{CHCl}_3$  were placed on top of each plate, and the plate was inverted and left to sit at room temperature for 10 min. The plates were then reinverted, and 3 mL of an albumin-dextrose-saline (ADS) solution [in g/L: NaCl, 8.1; bovine serum albumin, 50; anhydrous dextrose, 20] was added to each plate. Plates were gently swirled and left sitting at room temperature for 30 min, swirling occasionally. The top agar was scraped off into a flask using a funnel, making sure to wash the sides of the funnel with ADS medium. The flask was then left to shake for 60 min in a 37°C water bath. The contents of the flask were then centrifuged at 10 000 g for 15 min at room temperature in a SS34 rotor of a Sorvall RC5C centrifuge (Thermo Scientific, Wilmington, DE, USA). The pellet was discarded and the supernatant centrifuged again at 28 000 g in the same rotor for 30 min at room temperature. The resulting supernatant was discarded leaving behind a small pellet. The pellet was resuspended in 0.5 mL of ADS medium per centrifuge tube. The tubes were then put on a shaking table at room temperature for several hours until the pellet was fully resuspended. The resulting pooled stock titration was measured to be  $10^{10}$  PFU/mL and kept stored at 4°C over the duration of the experiment.

Before each test, the nebulizer was filled with model organisms suspended in solution. For the bacteriophage tests, 1 mL of T4 phage stock ( $\sim 10^{10}$  PFU) was added to the nebulizer and then the volume was completed to 30 mL using phage buffer (20 mM Tris-HCl, pH 7.5, 100 mM NaCl, 10 mM  $\text{MgSO}_4$ ). Similarly, for the bacterial tests, the nebulizer was filled with 10 mL of *E. coli* cell culture (optical density at 600 nm =  $1.0 \sim 1.0 \times 10^9$  cells/mL), which had been collected by centrifugation (as described above) and resuspended in 30 mL of phosphate-buffered saline (PBS, pH 7.4; 140 mM NaCl; 2.7 mM KCl; 10 mM  $\text{Na}_2\text{HPO}_4$ ; and 1.8 mM  $\text{KH}_2\text{PO}_4$ ), yielding a final concentration of about  $10^{10}$  cells/30 mL. Both buffer solutions are similar to the inorganic solutions that were used in a recent model organism aerosolization study.<sup>45</sup> Moreover, the mass fraction of the solute used in both buffer solutions was approximately 1%, which is consistent with the composition of human saliva, sputum, and exhaled droplets in that they are approximately 99% (or more) water.<sup>9,56,57</sup> Thus, the degree of evaporation of droplets from the bioaerosol emission source should be relatively similar to that for human respiratory emissions. For both organisms, all 30 mL of suspension was loaded into the nebulizer at the start of each trial. Aerosolization and simultaneous bioaerosol sampling continued for a total of 4 h for each test condition.

## 2.4 | Bioaerosol sampling

Active bioaerosol sampling was conducted in multiple locations throughout the apartment unit. Air sampling utilized five-stage Sioutas Personal Cascade Impactors (SKC, Inc., Eighty Four, PA, USA) operating at 9 L/min for 4-5 h to collect sufficient DNA for analysis. This allowed for particle collection within 5 size ranges of aerodynamic diameter: >2.5  $\mu\text{m}$ , 1.0-2.5  $\mu\text{m}$ , 0.5-1.0  $\mu\text{m}$ , and 0.25-0.5  $\mu\text{m}$ , all captured on 25-mm PTFE filters, as well as <0.25  $\mu\text{m}$  captured on 37-mm after-filters. Active bioaerosol sampling was conducted in four locations: approximately 0.5 m ("near-range"), 3 m ("short-range"), 5 m ("mid-range"), and 7 m ("long-range") in linear direction from the cough source (Figure 1). Passive bioaerosol sampling was also conducted using settle plates installed at three different distances from the source: 0.5 m away at floor height, 3 m away at 0.5 m height, and 5 m away at 1.7 m height. The settle plates were swabbed (Isohelix Buccal Swabs, MIDSCI, Valley Park, MO, USA) for 10 s across the width of each plate. Both the swabs and air sampler filters were collected immediately after testing and either processed successively after collection or frozen at -80°C for no more than 24 h.

## 2.5 | Filter and DNA extraction

The total genomic DNA was extracted from the PTFE filters by first cutting the filters into thirds, placing them into PowerBead tubes supplied with the PowerSoil DNA kit (MoBio Laboratories, Solana Beach, CA, USA), and then continuing following the manufacturer's instructions. The final elution step was modified by decreasing the total elution volume to 30  $\mu\text{L}$ . Template DNA concentration from each filter was measured using a Nanodrop2000c spectrophotometer (Thermo Scientific) and determined to be approximately 50 ng/ $\mu\text{L}$ . The DNA solutions were stored at -80°C for downstream use.

## 2.6 | Quantitative PCR amplification

Quantitative PCR was used to quantify the concentrations of the model organisms collected on both the air sampler filters and the settle plates. Negative controls were also included in each experimental run for each condition. Each reaction volume was a total of 25  $\mu\text{L}$ , containing 12.5  $\mu\text{L}$  of SYBR Green JumpStart Taq ReadyMix (Sigma, Saint Louis, MO, USA), 0.2  $\mu\text{L}$  of each primer (final concentration of 100 nM), 2  $\mu\text{L}$  of DNA template (approximate mass of 100 ng), and nuclease-free water. Thermal cycling was initiated by pre-heating at 94°C for 2 min, followed by 40 cycles of 94°C for 15 s and annealing temperature (dependent on primers) for 1 min at 72°C. The specific primers used in this study (IDT, Coralville, IA, USA), their sequences, and the annealing temperatures for each of the primers pairs are shown in Table 1. Both qPCR and data analysis were performed in an ABI PRISM 7700 real-time cycler (Applied Biosystems, Foster City, CA, USA) equipped with sequence detection system software.

All samples, including non-template controls, were measured in duplicates. Standard curves for quantifying the organisms were obtained following the method described by Arnaldos et al. (2013).<sup>58</sup> The DNA

**TABLE 1** Specific qPCR primers used in this study

Group	Primer	Sequence (5'-3')	Annealing Temp (°C)	Amplicon Length (bp)	Reference
<i>E. coli</i> K12	uidA-F	CAA CGA ACT GAA CTG GCA GA	60°C	100	Chern et al. (2011) <sup>59</sup>
	uidA-R	CAT TAC GCT GCG ATG GAT			
T4	T4F	CCA TCC ATA GAG AAA ATA TCA GAA CGA	59°C	120	Ninove et al. (2011) <sup>60</sup>
	T4R	GAA TGC ATC CAA ATC ATC AGC CAC			

was diluted to attain masses from 0.01 to 1000 ng; strong correlations ( $R^2 > 0.9$ ) were found between log mass values and cycle number to reach a threshold of fluorescence. Primer specificity and absence of primer-dimers were confirmed via melt-curve analysis, which was performed for every qPCR assay. The negative controls never yielded a reading above 0.1 ng and therefore were treated as negligible for each test run.

## 2.7 | Air exchange rate, temperature, and relative humidity measurements

For each trial performed in the test space, an Onset HOBO data logger was used to log indoor air temperature and relative humidity. To measure the air exchange rate (AER), CO<sub>2</sub> was injected into the test space for 15 min at the start of each trial, usually reaching ~1500 ppm inside. The subsequent decay was measured by two CO<sub>2</sub> monitors (PP Systems SBA-5; ±20 ppm accuracy) operated adjacent to the HVAC unit in the living room, both logging at 30-s intervals. One measured indoor CO<sub>2</sub> concentrations and the other measured outdoor CO<sub>2</sub> concentrations through a small outlet in the window. The AER was estimated by regressing the natural logarithm of the tracer gas concentrations (indoors minus outdoors) vs time.<sup>61</sup> All measurements were conducted at the start of each trial, and the data were averaged over the duration of each experiment.

## 2.8 | Bioaerosol resuspension test

Finally, resuspension of bioaerosols has been shown to have an important impact on indoor microbial concentrations.<sup>62-65</sup> One recent simulation study suggested that the resuspension of influenza viruses from a floor by walking could lead to meaningful exposures.<sup>66</sup> To test the likelihood of resuspension being a source of previously settled pathogens, we conducted a single experiment to estimate the magnitude of bioaerosol resuspension in the apartment unit. We first

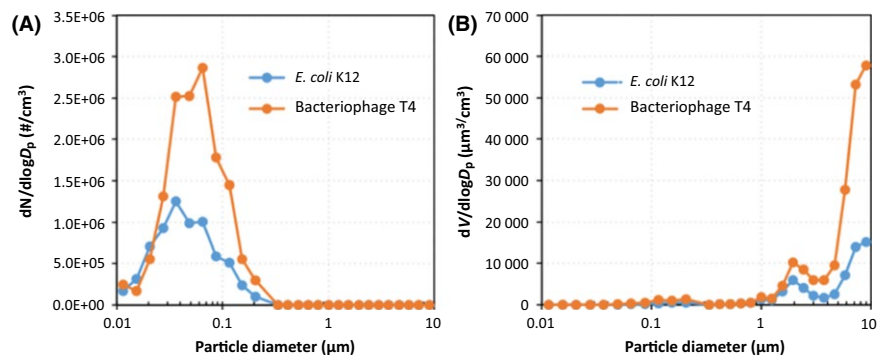
aerosolized both organisms, *E. coli* first and T4 second, following the same procedures as all other experiments, and then let the particles settle overnight. The next morning, air sampling was conducted for 4 h and five areas of the floor were swabbed, including immediately below the cough apparatus and also on the floor at the site of each of the 4 air samplers, to establish background concentrations. Next, two people walked in the apartment unit continuously for 5 h with the HVAC system operating without a filter, while each of the air samplers was operated continuously for the 5-h duration. The resulting concentrations were compared to background concentrations to characterize the extent of bioaerosol resuspension from the floor.

## 3 | RESULTS AND DISCUSSION

### 3.1 | Direct measurements of bioaerosol emissions

Figure 3 shows the resulting average particle size distributions in excess of background concentrations on both a number and volume basis (assuming spherical particles to estimate volume) measured within ~0.3 m of the bioaerosol emission source during initial *E. coli* and T4 experiments. Results are averaged over a combination of both constant low-flow “breathing” and periodic high-flow “coughing.” The size distributions with both organisms had peak number concentrations between 40 and 70 nm, but peak volume concentrations were between 5 and 10 μm. The resulting size-resolved number and volume distributions are reasonably well aligned with recently developed cough simulators<sup>42,51</sup> and with the small number of studies that have investigated particle size distributions resulting from human respiratory emissions using aerosol monitoring equipment that can measure below ~0.3 μm.<sup>4</sup> Given that the mass fraction of nonvolatile components is approximately 1%, the fully desiccated particle diameter would be expected to be only ~22% of the original emitted particle diameter.<sup>9</sup> This suggests that most of the mass of

**FIGURE 3** Particle size distributions in excess of background concentrations approximately 0.3 m from the bioaerosol emission source measured on a (A) number and (B) volume basis (assuming spherical particles)



each organism recovered in the air samples (at equilibrium) is likely to be in the ~1-2  $\mu\text{m}$  size range (assuming that complete desiccation occurs and only minimal evaporation has occurred in the volume distributions in Figure 3).

### 3.2 | Environmental conditions and ventilation rate measurements

A summary of air exchange rates (ACH), temperature, and relative humidity (RH) measured during each replicate test are shown in Table 2. Air exchange rates varied between ~0.5 and ~1 per h for most tests. Temperature and RH were both relatively consistent across all tests, although both were somewhat higher during the *E. coli* tests (ie, average of ~25°C and ~55% compared to ~22°C and ~52%).

### 3.3 | Bioaerosol transport measurements without HVAC filtration

We first explore the results from airborne size-resolved sampling of *E. coli* K12 and bacteriophage T4 under the no filter condition to characterize baseline aerosol transport in the apartment unit. Figure 4 shows that under the no filter conditions, *E. coli* K12 DNA was detected in all four sampling locations, decreasing from an average of ~120  $\text{ng}/\text{m}^3$  recovered from all size fractions combined in the near-range air sampling location (ie, 0.5 m away from the source) to <2  $\text{ng}/\text{m}^3$  recovered from all size fractions in the long-range air sampling location (ie, 7 m away from the source). For the near-range sampler, the vast majority of the mass of *E. coli* DNA recovered was found in the size fractions larger than 0.5  $\mu\text{m}$  (more than 97% of the mass), with 31% of the mass recovered in the >1  $\mu\text{m}$  size fraction.

Similarly, in the short-range sampler, approximately 99% of the recovered mass was found in size fractions >0.5  $\mu\text{m}$ , with ~28% in the size fraction larger than 1  $\mu\text{m}$ . However, more mass was recovered in the smaller size fractions from the mid-range and long-range samplers. In the mid-range sampler, ~85% of the recovered mass was found in size fractions >0.5  $\mu\text{m}$  (and 62% were >1  $\mu\text{m}$ ), while ~62% of the mass was recovered in the >0.5  $\mu\text{m}$  size fractions (and 44% were >1  $\mu\text{m}$ ) in the long-range sampler. These data demonstrate that although the average characteristic size of this organism is ~1  $\mu\text{m}$ , much of its DNA was found in submicron aerosol fractions in all locations in the room. This may be due to a combination of desiccation that reduces its characteristic size and/or fragmentation that occurs during the aerosolization process, both of which would influence the organism's viability in ways that qPCR would not be able to detect.

Somewhat similarly, Figure 5 shows that under the no filtration conditions, bacteriophage T4 DNA was also recovered in all airborne sampling locations, decreasing from an average of ~170  $\text{ng}/\text{m}^3$  recovered from all size fractions combined in the near-range air sampling location to ~3  $\text{ng}/\text{m}^3$  recovered from all size fractions in the long-range air sampling location. However, because bacteriophage T4 is a much smaller organism (~60 nm in characteristic size), the majority of its DNA was recovered in the submicron size fractions at all sampling locations. In the near-source location, approximately 49% of the mass was recovered in the size fractions smaller than 0.5  $\mu\text{m}$  and 90% was recovered from the <1  $\mu\text{m}$  size fractions. Similarly, in the long-range location, approximately 55% of the total mass was recovered from the <0.5  $\mu\text{m}$  size range and ~87% was recovered from the <1  $\mu\text{m}$  size fractions. There was not a substantial shift in the size distributions of mass recovered for bacteriophage T4 at any of the air sampling locations, which suggests that this smaller

**TABLE 2** Summary of air exchange rates (ACH), temperature, and relative humidity (RH) measured during each test

	<i>E. coli</i> K12			Bacteriophage T4		
	ACH, per h	Temperature, °C	RH (%)	ACH, per h	Temperature, °C	RH (%)
No filter	1.1	28	54	1.1	22	52
	1.0	28	55	0.8	23	51
	0.9	26	54	0.9	21	54
Average	1.0	27	54	0.9	22	52
MERV 8	0.5	23	53	1.1	24	52
	0.7	25	53	0.8	23	51
	0.4	23	56	0.9	22	54
Average	0.5	24	54	0.9	23	52
MERV 11	0.8	26	54	0.7	22	52
	0.8	27	56	0.8	23	51
	0.9	25	58	0.9	21	54
Average	0.8	26	56	0.8	22	52
MERV 16	0.5	25	56	0.7	22	52
	0.6	25	53	0.8	23	51
	0.5	26	56	0.9	21	54
Average	0.5	25	55	0.8	22	52

**FIGURE 4** (A) Average and standard deviations of size-resolved mass concentrations and (B) average relative proportion of mass recovered of *E. coli* K12 from four air sampling locations across three replicate tests without any HVAC particle filtration installed

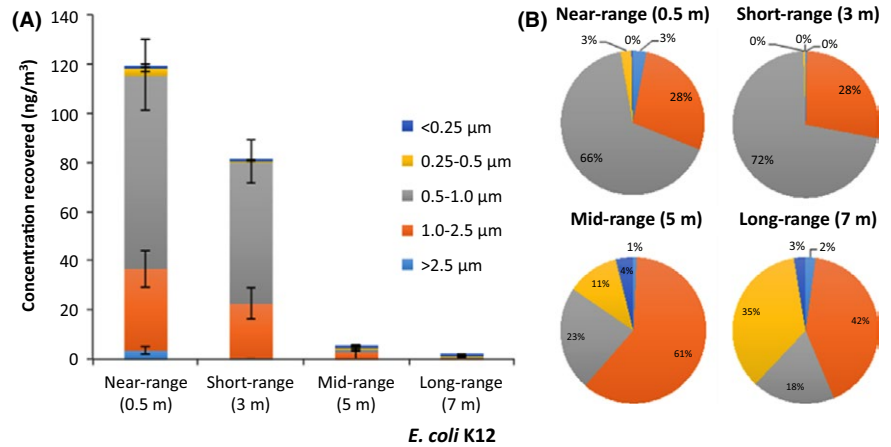
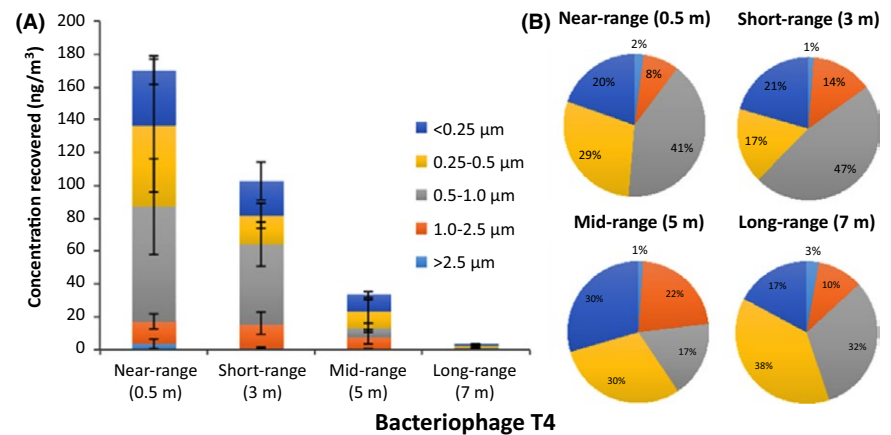


**FIGURE 5** (A) Average and standard deviations of size-resolved mass concentrations and (B) average relative proportion of mass recovered of bacteriophage T4 from four air sampling locations across three replicate tests without any HVAC particle filtration installed



organism is initially aerosolized in a smaller size fraction of droplets and remains suspended in a similar size distribution throughout the apartment unit.

Both the *E. coli* and bacteriophage results suggest that although the vast majority of particles aerosolized from the emission source are smaller than  $0.1 \mu\text{m}$  on a number basis and larger than  $5 \mu\text{m}$  on a volume basis (Figure 3), most of the airborne mass of DNA was detected in the  $0.25$  to  $2.5 \mu\text{m}$  size ranges (with a slight shift toward smaller size ranges for the smaller bacteriophage). This has implications for airborne infectious disease transmission studies, as it supports the use of sub- $1\text{-}\mu\text{m}$  or sub- $2.5\text{-}\mu\text{m}$  surrogates in bioaerosol transport models.<sup>40,67,68</sup>

In addition to the air samplers, three settle plates were also used to illustrate bioaerosol deposition to surfaces in the no filter condition. Figure 6 shows that the amount of *E. coli* K12 DNA recovered from each settle plate surface decreased proportionally with distance from the emission source. An average ( $\pm$  SD) of  $\sim 187 \text{ ng}$  ( $\pm 86 \text{ ng}$ ) was recovered from the near-range, floor height settle plate;  $\sim 122 \text{ ng}$  ( $\pm 58 \text{ ng}$ ) was recovered from the short-range, 0.5-m high settle plate; and  $\sim 20 \text{ ng}$  ( $\pm 5 \text{ ng}$ ) was recovered from the mid-range, 1.7-m high settle plate. In contrast, the largest concentration of bacteriophage T4 DNA was recovered from the short-range settle plate ( $\sim 79 \pm 25 \text{ ng}$ ), and the smallest amount was recovered from the settle plate closest to the source ( $\sim 6 \pm 2 \text{ ng}$ ). This illustrates that surface deposition for each organism was highly varied, likely because the varying size of each

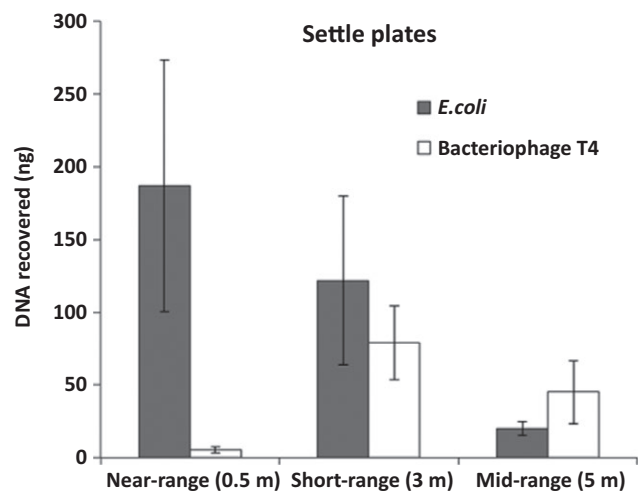


**FIGURE 6** DNA recovered from settle plates in three locations with the recirculating HVAC system on without a filter installed. Near-range (0.5 m) plates were installed at floor height; short-range (3 m) at 0.5 m height; and mid-range (5 m) at 1.7 m height. Values represent average and standard deviations across three replicate tests

organism influenced the sizes of the initial emitted aerosols in which they were contained and thus altered the distance that it was able to travel from the source.

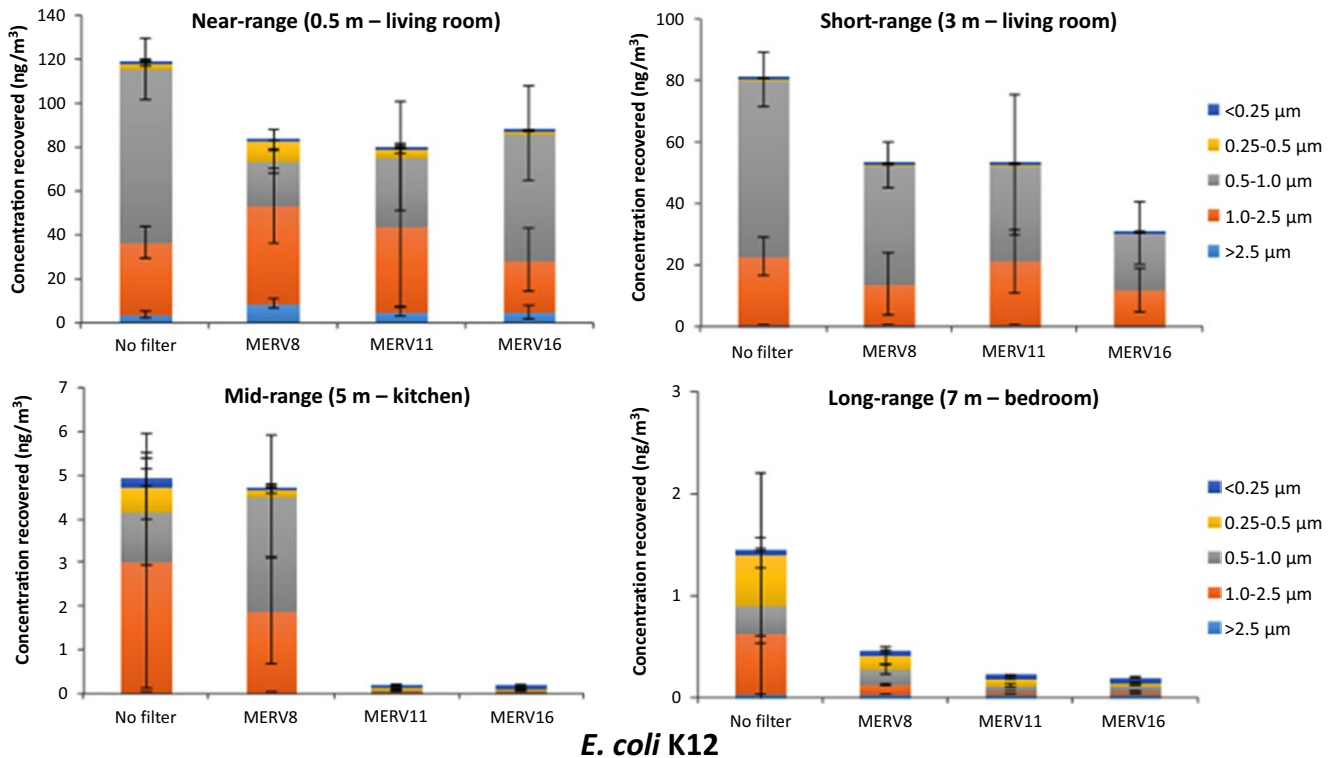


**FIGURE 7** Mass concentrations of *E. coli* K12 DNA recovered and amplified from the four air sampling locations with four levels of HVAC filtration installed. Values represent average and standard deviations across three replicate tests

### 3.4 | Bioaerosol control measurements with HVAC particle filtration

Figure 7 shows results for the total and size-resolved mass concentrations of *E. coli* DNA recovered in the air samples under each of the four filter conditions: no filter, MERV 8, MERV 11, and MERV 16. Increased HVAC filtration efficiency had small or negligible impacts on the amount of *E. coli* DNA amplified from the near-range and short-range air samplers, but had a greater impact on the longer-range samplers. Compared to the no filter condition, there was an average reduction in total *E. coli* mass concentration recovered in the mid-range sampler of ~4%, ~96%, and ~97% with MERV 8, 11, and 16 filters installed, respectively, and average reductions of ~69%, ~85%, and ~87% in the long-range sampler.

Figure 8 shows similar results for bacteriophage T4 recovery from air samples with different HVAC filter conditions. There was an average reduction in the total mass concentration of bacteriophage T4 DNA recovered and amplified in the mid-range air sampler of ~70%, ~93%, and ~98% with the MERV 8, 11, and 16 filters installed, respectively, and reductions of ~12%, ~81%, and ~92%, respectively, in the long-range air sampler.

Figure 9 shows the same data for both organisms plotted vs the distance from the source and normalized to the total amount of DNA recovered in the closest (ie, near-range) air sampler to more clearly demonstrate the impact of distance. There was a large decrease in the total amount of DNA recovered across all particle sizes under all four filtration conditions beginning approximately 3 m away from the

source. These data also demonstrate that MERV 8 filters were not particularly effective for controlling long-range bioaerosol transport for both organisms, but that both MERV 11 and MERV 16 had greater impacts. Further, the difference between MERV 16 and MERV 11 filtration was greater at longer distances for the smaller bacteriophage T4 than for the larger *E. coli* K12.

Similarly, Figure 10 shows the amount of DNA recovered and amplified for both model organisms from the three settle plate locations under each of the four HVAC filter conditions. For *E. coli* K12, the greatest amount of DNA recovery was found on the near-range settle plates and higher efficiency HVAC filtration had a small or negligible impact on the amount of DNA amplified from that plate. However, increased HVAC filtration efficiency reduced the amount of *E. coli* DNA recovered from both the short-range and mid-range settle plates, although the amount of *E. coli* DNA amplified from the mid-range settle plates was consistently very low. Conversely, very little bacteriophage T4 DNA was amplified from the near-range settle plate under any HVAC filter condition, further suggesting that this smaller organism remained encapsulated in droplets as they evaporated, reduced in size to droplet nuclei, and were mostly transported longer distances. Further evidence of this is that increased HVAC filter efficiency also reduced bacteriophage T4 DNA recovery on both the short-range and mid-range settle plates.

### 3.5 | Resuspension test

Finally, results from the single resuspension test did not reveal meaningful resuspension of either bacteriophage T4 or *E. coli*. Although

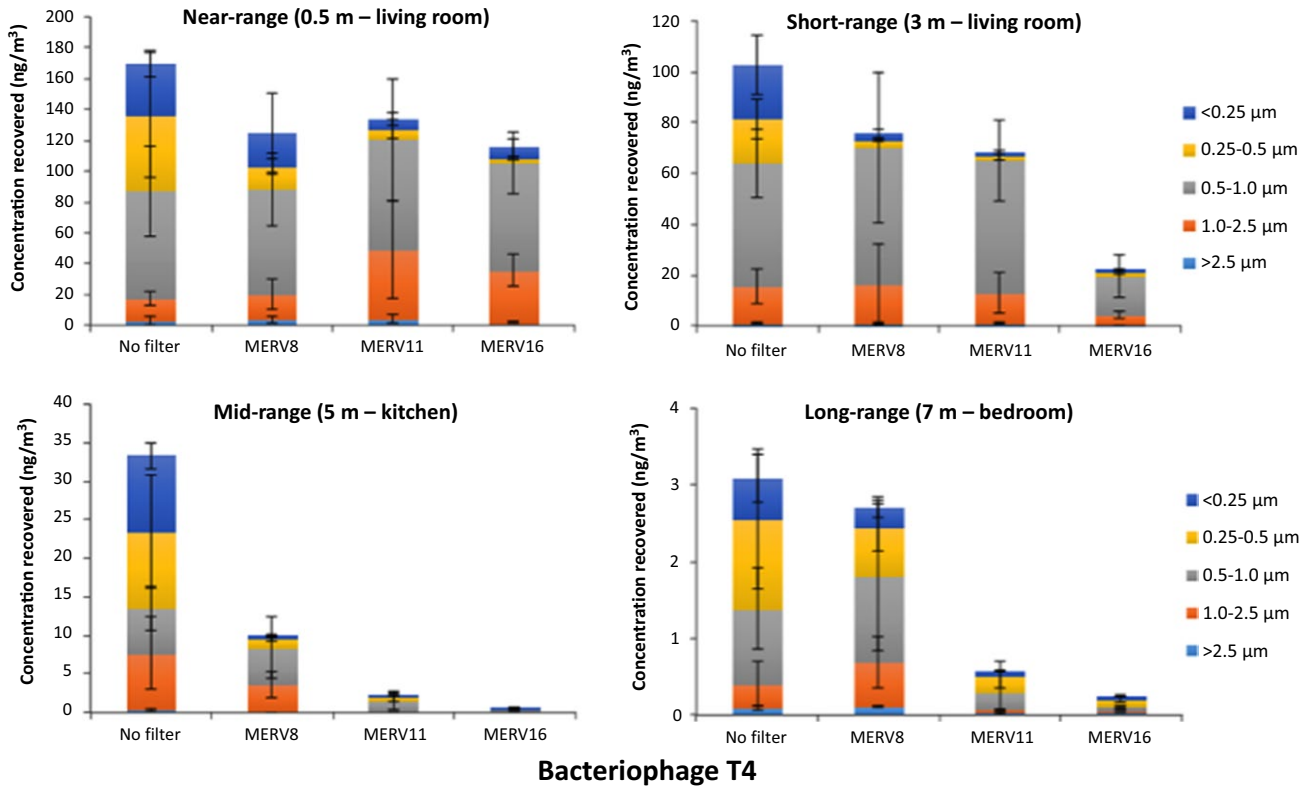


**FIGURE 8** Mass concentrations of bacteriophage T4 DNA recovered and amplified from the four air sampling locations with four levels of HVAC filtration installed. Values represent average and standard deviations across three replicate tests.

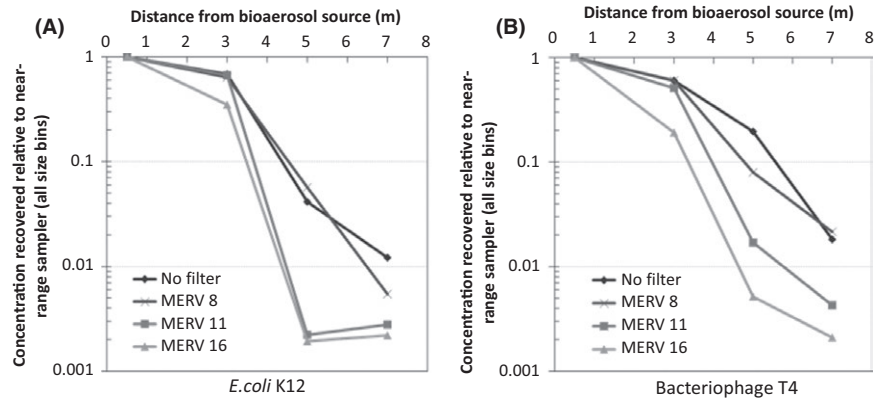


**FIGURE 9** Relative mass concentrations for (A) *E. coli* K12 and (B) bacteriophage T4 DNA recovered and amplified from air samplers (all size fractions combined) under four HVAC filtration conditions as a function of distance from the bioaerosol source. Values represent averages across three replicate tests

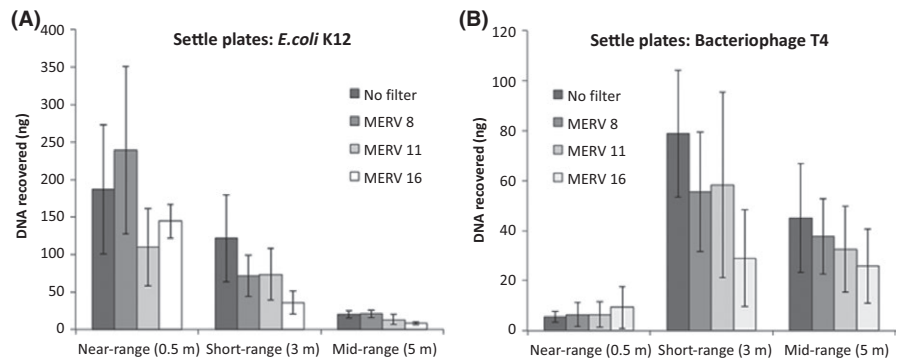


**FIGURE 10** Total DNA recovered and amplified from surface sampling at three locations under four HVAC filter conditions for *E. coli* K12 and bacteriophage T4. Near-range (0.5 m) plates were installed at floor height; short-range (3 m) at 0.5 m height; and mid-range (5 m) at 1.7 m height. Values represent average and standard deviations across three replicate tests

there was a measurable amount of DNA recovered for both organisms from the floor samples prior to walking, particularly within close range of the bioaerosol emission source, DNA recovery from the air samples was below detection limits. This demonstrates that the impact of resuspension on the measured bioaerosol concentrations for this experimental setup were negligible. However, these results should be confirmed in other settings before drawing meaningful conclusions from these data.

## 4 | CONCLUSION

To our knowledge, this is one of the first studies to experimentally quantify the size-resolved aerosol dynamics of surrogate microorganisms emitted in a realistic indoor environmental setting under varying HVAC filtration conditions. Results demonstrate that both *E. coli* K12 and bacteriophage T4 DNA were recovered and amplified in air samples up to 7 m away under all filtration conditions, albeit in much smaller amounts than in near-source samples. Higher efficiency HVAC particle filtration (eg, MERV 11 and MERV 16) clearly reduced the recoverable amount of DNA from both organisms in air samples and on settle plates located ~3 to ~7 m away from the source. Moreover, the characteristic size of the model organisms also influenced the particle size range in which their DNA was detectable, as a greater fraction of the recoverable T4 DNA was found in submicron aerosol size fractions than *E. coli* K12 at all distances from the source. These results provide insight into how the size-resolved aerosol dynamics of potentially pathogenic organisms emitted from respiratory activities may influence their transmission and control in indoor environments.

## ACKNOWLEDGEMENTS

Stephanie Kunkel was funded by a Microbiology of the Built Environment (MoBE) Postdoctoral Fellowship from the Alfred P. Sloan Foundation (Grant No. G-2013-5-25 MBPF). Brent Stephens was also funded in part by an ASHRAE New Investigator Award.

## REFERENCES

- Fisk WJ. Health and productivity gains from better indoor environments and their relationship with building energy efficiency. *Annu Rev Energy Environ*. 2000;25:537-566.
- Yang S, Lee GWM, Chen C-M, Wu C-C, Yu K-P. The size and concentration of droplets generated by coughing in human subjects. *J Aerosol Med Off J Int Soc Aerosols Med*. 2007;20:484-494.
- Johnson GR, Morawska L, Ristovski ZD, et al. Modality of human expired aerosol size distributions. *J Aerosol Sci*. 2011;42:839-851.
- Holmgren H, Ljungström E, Almstrand A-C, Bake B, Olin A-C. Size distribution of exhaled particles in the range from 0.01 to 2.0  $\mu\text{m}$ . *J Aerosol Sci*. 2010;41:439-446.
- Fabian P, Brain J, Houseman EA, Gern J, Milton DK. Origin of exhaled breath particles from healthy and human rhinovirus-infected subjects. *J Aerosol Med Pulm Drug Deliv*. 2011;24:137-147.
- Morawska L, Johnson GR, Ristovski ZD, et al. Size distribution and sites of origin of droplets expelled from the human respiratory tract during expiratory activities. *J Aerosol Sci*. 2009;40:256-269.
- Xie X, Li Y, Sun H, Liu L. Exhaled droplets due to talking and coughing. *J R Soc Interface*. 2009;6:S703-S714.
- Nardell EA. Chapter 11: Disinfecting air. *Indoor Air Quality Handbook*. New York, NY: McGraw-Hill; 2001.
- Nicas M, Nazaroff WW, Hubbard A. Toward understanding the risk of secondary airborne infection: emission of respirable pathogens. *J Occup Environ Hyg*. 2005;2:143-154.
- Verreault D, Moineau S, Duchaine C. Methods for sampling of airborne viruses. *Microbiol Mol Biol Rev*. 2008;72:413-444.
- Boone SA, Gerba CP. The prevalence of human parainfluenza virus 1 on indoor office fomites. *Food Environ Virol*. 2010;2:41-46.
- Boone S, Gerba C. The occurrence of influenza A virus on household and day care center fomites. *J Infect*. 2005;51:103-109.
- Jones RM, Adida E. Influenza infection risk and predominate exposure route: uncertainty analysis. *Risk Anal*. 2011;31:1622-1631.
- Alford RH, Kasel JA, Gerone PJ, Knight V. Human influenza resulting from aerosol inhalation. *Exp Biol Med*. 1966;122:800-804.
- Bean B, Moore BM, Sterner B, Peterson LR, Gerding DN, Balfour HH. Survival of influenza viruses on environmental surfaces. *J Infect Dis*. 1982;146:47-51.
- Riley RL. Indoor airborne infection. *Environ Int*. 1982;8:317-320.
- Chen C, Zhao B. Some questions on dispersion of human exhaled droplets in ventilation room: answers from numerical investigation. *Indoor Air*. 2010;20:95-111.
- Yang W, Marr LC. Dynamics of airborne influenza A viruses indoors and dependence on humidity. *PLoS ONE*. 2011;6:e21481.
- Dick EC, Jennings LC, Mink KA, Wartgow CD, Inborn SL. Aerosol transmission of rhinovirus colds. *J Infect Dis*. 1987;156:442-448.
- Spicknall IH, Koopman JS, Nicas M, Pujol JM, Li S, Eisenberg JNS. Informing optimal environmental influenza interventions: how the host, agent, and environment alter dominant routes of transmission. *PLoS Comput Biol*. 2010;6:e1000969.
- Azimi P, Stephens B. HVAC filtration for controlling infectious airborne disease transmission in indoor environments: Predicting risk reductions and operational costs. *Build Environ*. 2013;70:150-160.
- Cowling BJ, Ip DKM, Fang VJ, et al. Aerosol transmission is an important mode of influenza A virus spread. *Nat Commun*. 2013;4:1935.
- ASHRAE. *ASHRAE Position Document on Airborne Infectious Diseases*. American Society of Heating, Refrigerating and Air-Conditioning Engineers; 2014.
- Schaal KP. Medical and microbiological problems arising from airborne infection in hospitals. *J Hosp Infect*. 1991;18:451-459.
- Warfel JM, Beren J, Merkel TJ. Airborne transmission of *Bordetella pertussis*. *J Infect Dis*. 2012;206:902-906.
- Greatorex JS, Digard P, Curran MD, et al. Survival of influenza A(H1N1) on materials found in households: implications for infection control. *PLoS ONE*. 2011;6:e27932.
- Fabian P, McDevitt JJ, DeHaan WH, et al. Influenza virus in human exhaled breath: an observational study. *PLoS ONE*. 2008;3:e2691.
- Blachere FM, Lindsley WG, Pearce TA, et al. Measurement of airborne influenza virus in a hospital emergency department. *Clin Infect Dis*. 2009;48:438-440.
- Lindsley WG, Blachere FM, Davis KA, et al. Distribution of airborne influenza virus and respiratory Syncytial virus in an urgent care medical clinic. *Clin Infect Dis*. 2010;50:693-698.
- Lindsley WG, Blachere FM, Thewlis RE, et al. Measurements of airborne influenza virus in aerosol particles from human coughs. *PLoS ONE*. 2010;5:e15100.
- Yang W, Elankumaran S, Marr LC. Concentrations and size distributions of airborne influenza A viruses measured indoors at a health centre, a day-care centre and on aeroplanes. *J R Soc Interface*. 2011;8:1176-1184.
- Bischoff WE, Swett K, Leng I, Peters TR. Exposure to influenza virus aerosols during routine patient care. *J Infect Dis*. 2013;207:1037-1046.

33. Lednicky JA, Loeb JC. Detection and isolation of airborne influenza A H3N2 virus using a sioutas personal cascade impactor sampler. *Influenza Res Treat*. 2013. doi:10.1155/2013/656825.
34. Milton DK, Fabian MP, Cowling BJ, Grantham ML, McDevitt JJ. Influenza virus aerosols in human exhaled breath: particle size, culturability, and effect of surgical masks. *PLoS Pathog*. 2013;9:e1003205.
35. Brosseau LM, Vesley D, Chen S-K, Gabel C, Kuehn TH, Goyal SM. Investigate and Identify Means of Controlling Virus in Indoor Air by Ventilation, Filtration or Source Removal. American Society of Heating, Refrigerating, and Air-Conditioning Engineers; 1994. Report No.: 776-RP.
36. Miller-Leiden S, Lohascio C, Nazaroff WW, Macher JM. Effectiveness of in-room air filtration and dilution ventilation for tuberculosis infection control. *J Air Waste Manag Assoc*. 1996;46:869-882.
37. Nazaroff WW, Nicas M, Miller SL. Framework for evaluating measures to control nosocomial tuberculosis transmission. *Indoor Air*. 1998;8:205-218.
38. RTI. Test Report of Filtration Efficiency of Bioaerosols in HVAC Systems. Research Triangle Institute; 2004; RTI Project No. 08787.001.
39. Fisk WJ, Seppanen O, Faulkner D, Huang J. Economic benefits of an economizer system: energy savings and reduced sick leave. *ASHRAE Trans*. 2005;111:673-679.
40. Emmerich SJ, Heinzerling D, Choi J, Persily AK. Multizone modeling of strategies to reduce the spread of airborne infectious agents in healthcare facilities. *Build Environ*. 2013;60:105-115.
41. Noti JD, Blachere FM, McMillen CM, et al. High humidity leads to loss of infectious influenza virus from simulated coughs. *PLoS ONE*. 2013;8:e57485.
42. Lindsley WG, King WP, Thewlis RE, et al. Dispersion and exposure to a cough-generated aerosol in a simulated medical examination room. *J Occup Environ Hyg*. 2012;9:681-690.
43. Noti JD, Lindsley WG, Blachere FM, et al. Detection of infectious influenza virus in cough aerosols generated in a simulated patient examination room. *Clin Infect Dis*. 2012;54:1569-1577.
44. Griffiths WD, Bennett A, Speight S, Parks S. Determining the performance of a commercial air purification system for reducing airborne contamination using model micro-organisms: a new test methodology. *J Hosp Infect*. 2005;61:242-247.
45. Turgeon N, Toulouse M-J, Martel B, Moineau S, Duchaine C. Comparison of five bacteriophages as models for viral aerosol studies. *Appl Environ Microbiol*. 2014;80:4242-4250.
46. Tung-Thompson G, Libera DA, Koch KL, de los Reyes FL, Jaykus L-A. Aerosolization of a human norovirus surrogate, bacteriophage MS2, during simulated vomiting. *PLoS ONE*. 2015;10:e0134277.
47. Smith JA, Aliverti A, Quaranta M, et al. Chest wall dynamics during voluntary and induced cough in healthy volunteers. *J Physiol*. 2012;590:563-574.
48. McCool FD. Global physiology and pathophysiology of cough: ACCP evidence-based clinical practice guidelines. *Chest*. 2006;129:485-535.
49. Hegland KW, Troche MS, Davenport PW. Cough expired volume and airflow rates during sequential induced cough. *Front Physiol*. 2013;4:167.
50. Gupta JK, Lin C-H, Chen Q. Flow dynamics and characterization of a cough: flow dynamics and characterization of a cough. *Indoor Air*. 2009;19:517-525.
51. Lindsley WG, Reynolds JS, Szalajda JV, Noti JD, Beezhold DH. A cough aerosol simulator for the study of disease transmission by human cough-generated aerosols. *Aerosol Sci Technol*. 2013;47:937-944.
52. ISO/TS. Respiratory protective devices - Human factors - Part 1: Metabolic rates and respiratory flow rates. 2015.
53. Zhao H, Stephens B. A method to measure the ozone penetration factor in residences under infiltration conditions: application in a multi-family apartment unit. *Indoor Air*. 2016;26:571-581.
54. Stephens B, Siegel JA, Novoselac A. Operational characteristics of residential and light-commercial air-conditioning systems in a hot and humid climate zone. *Build Environ*. 2011;46:1972-1983.
55. Fazli T, Stephens B. Characterizing the in-situ size-resolved removal efficiency of residential HVAC filters for fine and ultrafine particles. *Proc 2016 ASHRAE Winter Conf*. Orlando, FL; 2016.
56. Humphrey SP, Williamson RT. A review of saliva: normal composition, flow, and function. *J Prosthet Dent*. 2001;85:162-169.
57. Spicer SS, Martinez JR. Mucin biosynthesis and secretion in the respiratory tract. *Environ Health Perspect*. 1984;55:193-204.
58. Arnaldos M, Kunkel SA, Stark BC, Pagilla KR. Enhanced heme protein expression by ammonia-oxidizing communities acclimated to low dissolved oxygen conditions. *Appl Microbiol Biotechnol*. 2013;97:10211-10221.
59. Chern EC, Siefing S, Paar J, Doolittle M, Haugland RA. Comparison of quantitative PCR assays for *Escherichia coli* targeting ribosomal RNA and single copy genes: qPCR assays for *E. coli* targeting rRNA and single copy genes. *Lett Appl Microbiol*. 2011;52:298-306.
60. Ninove L, Nougairede A, Gazin C, et al. RNA and DNA bacteriophages as molecular diagnosis controls in clinical virology: a comprehensive study of more than 45,000 routine PCR tests. *PLoS ONE*. 2011;6:e16142.
61. ASTM E741. Standard test method for determining air change in a single zone by means of a tracer gas dilution. 2006.
62. Karlsson E, Fångmark I, Berglund T. Resuspension of an indoor aerosol. *J Aerosol Sci*. 1996;27:S441-S442.
63. Karlsson E, Berglund T, Strömqvist M, Nordstrand M, Fångmark I. The effect of resuspension caused by human activities on the indoor concentration of biological aerosols. *J Aerosol Sci*. 1999;30:S737-S738.
64. Hambræus A, Bengtsson S, Laurell G. Bacterial contamination in a modern operating suite. 3. Importance of floor contamination as a source of airborne bacteria. *J Hyg*. 1978;80:169-174.
65. Gomes C, Freihaut J, Bahnfleth W. Resuspension of allergen-containing particles under mechanical and aerodynamic disturbances from human walking. *Atmos Environ*. 2007;41:5257-5270.
66. Khare P, Marr LC. Simulation of vertical concentration gradient of influenza viruses in dust resuspended by walking. *Indoor Air*. 2015;25:428-440.
67. He Q, Niu J, Gao N, Zhu T, Wu J. CFD study of exhaled droplet transmission between occupants under different ventilation strategies in a typical office room. *Build Environ*. 2011;46:397-408.
68. Mui KW, Wong LT, Wu CL, Lai ACK. Numerical modeling of exhaled droplet nuclei dispersion and mixing in indoor environments. *J Hazard Mater*. 2009;167:736-44.

**How to cite this article:** Kunkel SA, Azimi P, Zhao H, Stark BC, Stephens B. Quantifying the size-resolved dynamics of indoor bioaerosol transport and control. *Indoor Air*. 2017;00:1-11. <https://doi.org/10.1111/ina.12374>